

A Porous Composites of Poly(ethylene glycol)-poly(ϵ – caprolactone) Nanomicelles and Chitosan for Curcumin Delivery

Thi Hong Anh Nguyen^{1,*}, Thi Thanh Hue Phan² and Van Cuong Nguyen²

¹Faculty of Chemical Engineering, Ho Chi Minh City University of Food Industry, Ho Chi Minh City 70000, Vietnam

²Faculty of Chemical Engineering, Industrial University of Ho Chi Minh City, Ho Chi Minh City 70000, Vietnam

*Corresponding author (e-mail: anhnh@hufi.edu.vn)

As a multi-functional drug, curcumin has a great potential for various applications in medicine. However, the use of curcumin is still limited owing to its high hydrophobicity, poor absorption, rapid metabolism, and rapid systemic elimination. Recently, the utilization of biodegradable polymers for curcumin delivery presents a promising approach to overcome these disadvantages. This study developed a drug delivery system using curcumin-encapsulated methoxy poly(ethylene glycol)-block-poly(-caprolactone) nanomicelles, which were then submerged in chitosan networks (cur-mPEC-C). Fourier-transform infrared (FTIR) spectrometry was employed to investigate the chemical structures of both micelles and nanocomposites. Morphologies of the nanocomposites were obtained through scanning electron microscope (SEM) analysis. The average particle size of micelles between 144 to 182 nm was measured by DLS. Cur-mPEC with the average particle size of 144 nm (ratio of mPEC/Curcumin 8:1) was utilized as the optimized sample for incorporating chitosan. Curcumin-loaded mPEC/chitosan nanocomposites were produced by freeze-drying method and characterized. The drug release profile revealed that chitosan enabled avoidance of the burst release of curcumin.

Keywords: Chitosan; nanomicelle; curcumin; mPEG–PCL; drug delivery system

Received: January 2023; Accepted: March 2023

Curcumin, a yellow pigment of turmeric (*Curcuma longa* L.), has been known as a bioactive compound to enhance effectiveness of drugs, such as antioxidants, antimicrobials, anticarcinogenics, anti-inflammatories, antiarthritics, enhance wound healing, and so on¹⁻⁴. Curcumin also has therapeutic benefits for skin health, food, and biotechnological applications⁵. Additionally, curcumin has also been shown in recent studies to have other potentials in cancer treatment⁶⁻⁸. However, curcumin has some drawbacks that limit its utility in clinical settings. For instance, curcumin has low bioavailability and solubility (at acidic or neutral pH), and a short half-life in plasma⁹. Curcumin can be rapidly decomposed in an alkaline medium^{10,11}. Most importantly, curcumin has been found to have poor absorption, rapid metabolism, high *in vivo* elimination rates, and inability to cross the stratum corneum to reach wounds^{12,13}.

Recently, nanosized drug delivery systems have proven to be crucial in delivering drugs in a targeted manner. Nanosized drug delivery systems improve efficacy, reduce side effects and clearance, increase cellular uptake, and prolong time in circulation. They have many advantages over free drugs, e.g., protecting drugs from premature degradation, preventing drugs from prematurely interacting with the biological environment, enhancing absorption of drugs into tumor tissues via the enhanced permeability and retention

effect (EPR), controlling drugs' pharmacokinetic and tissue distribution profiles, and improving intracellular penetration¹⁴.

Many effective techniques and approaches, such as encapsulation into nanoparticles, liposomes, micelles, phospholipid complexes, electrospraying, local drug delivery, and gelation, have been used to overcome the problems^{15,16}. Among them, micelles can improve the gastrointestinal absorption of natural drugs, resulting in higher plasma levels and lower kinetic elimination, thereby improving bioavailability¹². Letchford and colleagues discovered that polymeric formulations containing methoxy poly(ethylene glycol)-block-poly(-caprolactone) copolymers (mPEG-*b*-PCL) can increase the solubility of curcumin up to 13×10^5 folds¹⁷, which attracted the enormous studies on these polymeric micelles. Nevertheless, the release of curcumin with mPEG-*b*-PCL occurs rapidly owing to the highly hydrophilic polymer segment of mPEG. Therefore, the development of hybrid micelles is considered a promising solution. Due to higher drug bioavailability, decreased drug cost, increased drug targeting, and decreased medication side effects, transdermal drug administration has shown the potential utility for curcumin delivery.

The objective of this study is to overcome the limitations of drug delivery by introduction of

curcumin into nanomicelles for drug delivery system; thus, a drug delivery system based on mPEG–PCL/chitosan was developed. Curcumin was encapsulated in mPEG-PCL micelles, which was then hybridized with chitosan to control the drug release profile. It is well-known that chitosan is rigid, insoluble, and stable owing to strong intermolecular hydrogen bonds, making it a promising carrier material^{18,19}.

EXPERIMENTAL

Chemicals and Materials

All reagents used were of analytical grade and used without further purification. Curcumin 95% was purchased from Marven Bio Chem (India); chitosan ($\geq 75\%$, deacetylated); and glutaraldehyde (50%) (GA) were obtained from Sigma Aldrich, Singapore. All the chemicals used for synthesizing mPEG-PCL, including ϵ -caprolactone (CL), tin(II) 2-ethylhexanoate Sn(Oct)₂, and methoxy polyethylene glycol (mPEG), were purchased from Sigma Aldrich, Singapore.

Preparation of Curcumin-loaded Methoxy Poly(ethylene glycol)-block-poly(ϵ -caprolactone) (cur-mPEC) Micelles

The mPEG–PCL diblock copolymer ($M_{n,PCL} = 22,000$) was successfully synthesized and characterized elsewhere²⁰. In brief, the mPEG–PCL diblock copolymers were synthesized by ring opening polymerization of ϵ -caprolactone in the presence of mPEG-OH as a macro-initiator with Sn(Oct)₂ serving as a catalyst. Predetermined amounts of mPEG-OH, ϵ -caprolactone, and Sn(Oct)₂ were added into a 250 mL three-necked flask under a nitrogen atmosphere and mechanical stirring. The resulting mixture was refluxed for 4 h at 130°C. After the reaction was completed, the mixture was dissolved in DCM and precipitated in diethyl ether: hexane (9:1, v/v). The product was filtered and dried in vacuum for 24 h to deliver mPEC copolymer. The critical micelle concentration value of mPEC was 5.1×10^{-4} mg/mL. A modified solvent extraction method using acetone as the solvent was used to prepare curcumin-loaded micelles²¹. Firstly, 10 mg of curcumin was dissolved in 6 mL of acetone (the amount of curcumin was kept constant throughout the study). Next, a calculated amount of mPEC (Table 1) was added to the curcumin solution, followed by 25 mL of deionized water. The organic solvents were removed by rotary evaporation and filtered through a Millipore 0.45 μ m filter to obtain the self-assembled micelles of the curcumin-encapsulated mPEC. The mass ratios of curcumin to mPEC are listed in Table 1. The particle size of prepared nanomicelles was measured using a particle size analyzer (LB-550, Horiba, Japan).

Preparation of Curcumin-loaded mPEG-PCL/Chitosan (cur-mPEC-C) Nanocomposites

Chitosan is able to protect drugs from harsh

environments and slows down the drug release rate²². Therefore, different amounts (0.1, 0.2, 0.7, and 2.5 g) of cur-mPEC micelles at optimum mass ratios were used to prepare cur-mPEC-C nanocomposites. Typically, chitosan solution 1.5% was obtained by dissolving 10 g of chitosan in 600 mL of CH₃COOH 1%. A prepared micelle was poured into 120 mL of chitosan solution under a continuous stirring of 600 rpm, and the mixture was stirred for further 1 h. Afterwards, 4 mL of glutaraldehyde (GA) 5% was added to the solution. The mixture was continuously stirred for 15 min. The product was transferred into a 50 mL Falcon tube and placed in a -40°C deep freezer for 24 h. The frozen samples were lyophilized for 48 h under a freeze dryer. The samples were then stored at room temperature for further experiments. The quantification of curcumin was measured by UV-Vis spectrophotometric method²³.

To confirm the presence of interactions between drug and polymer, and chitosan as well, the Fourier-transform infrared (FTIR) spectroscopic spectra of pure curcumin, diblock copolymer, chitosan, and the nanocomposites were recorded from 500 cm⁻¹ to 4000 cm⁻¹. The morphologies of the micelles, as well as that of the nanocomposites, were measured by scanning electron microscope (SEM) technique.

Drug Encapsulation Efficiency

Drug encapsulation efficiency is defined as the weight percentage of curcumin in micelles relative to the initial feeding amount of curcumin. The amount of curcumin loaded in the micelles was determined by the absorption at 420 nm using UV-Vis spectrometry²³. Curcumin solutions of various concentrations were prepared, and the absorptions of the solutions were measured to obtain a calibration curve.

Drug Release Profile

The release of curcumin from the nanocomposites was carried out at pH = 7.4 and 5. These two pH values were used to mimic the pH gradient from the stomach to the intestine²⁴. 100 mg of freeze-dried nanocomposite was dissolved in 10 mL of PBS solution and incubated at 37°C. Then, at determined time intervals, 3 mL of the solution was taken out and replaced by 3 mL of fresh PBS. The concentration of the released curcumin was measured using an ultra-violet-visible (UV-Vis) spectrophotometer at the wavelength of 420 nm.

Statistical Analysis

All experiments were conducted in triplicate. Statistical analyses were performed by the Student's test. Statistical differences were considered to be significant when *P*-value was less than 0.05. Results are calculated and presented as mean \pm standard deviation. The curcumin calculation method was validated by our laboratory before being applied to the

analysis of curcumin. In detail, correlation coefficient (R^2), relative standard deviation (RSD, %), and recovery (%) are 0.99, 2.85% and 94-102%, respectively.

RESULTS AND DISCUSSION

Preparation of Cur-mPEC Micelles

The amphiphilic mPEC with the longer hydrophobic segment (PCL) was used to encapsulate curcumin due to its hydrophobicity¹². As seen in Figure 1, cur-mPEC micelles only formed at the mass ratio range of 8:1 – 12:1. The reason behind this is curcumin could be physically encapsulated into copolymeric nanoparticles due to the hydrophobic interaction between the drug and the PCL core²². For cur-mPEC-4 and cur-mPEC-6 samples, the mPEC distributed throughout the solutions and acted as a surfactant. It adsorbed at the aqueous-organic solvent interface (DI water-acetone in this study) instead of interacting with curcumin to form micelles due to the insufficient number of copolymer chains. With increasing amounts of mPEC, the adsorbed mPEC at the interface increased, resulting in the interaction between mPEC and curcumin molecules to produce the micelles (cur-

mPEC-8, cur-mPEC-10, and cur-mPEC-12). As the amount of mPEC reached the saturated point (cur-mPEC-15), the micelles became unstable and resulted in disassembling, releasing free chains that could be adsorbed again at the interface²⁵. Similar explanations for the average size and that of the particle size distribution of cur-mPEC micelles were considered. The curcumin encapsulation efficiency increased with the increase of mPEC amount. The curcumin encapsulation efficiencies were 33.6, 38.3, and 41.2 for Cur-mPEC-8, Cur-mPEC-10, and Cur-mPEC-12, respectively (Table 1). The high encapsulation efficiency of curcumin into SEDDS and α -tocopherol nanoemulsion has also been reported^{26,27}. From the results in Table 1 and Figure 2, the particle size increased with the increase in the mass ratio of mPEC. Cur-mPEC-8 obtained the minimal average particle size of 144 nm, which was chosen as the optimum micelles since there was no precipitation. The *in vitro* stability of Cur-mPEC-8 was investigated at 37°C. The size of Cur-mPEC-8 was evaluated via DLS measurements for a period of up to 7 days. The result was, Cur-mPEC-8 retained its size over the 7 days incubation period. This could be attributed to the high CMC value of mPEC.



Figure 1. Image of micellar formulations with mass ratios of mPEC to curcumin of 4:1 to 15:1 (left to right).

Table 1. Compositions and particle sizes of prepared curcumin/mPEC.

No.	Abbreviation	mPEC (mg)	Curcumin (mg)	mPEC/ Curcumin mass ratio	Encapsulation efficiency (%)	Average diameter (nm)	PDI	Zeta potential (mV)
1	Cur-mPEC-4	40	10	4:1	-	-	-	-
2	Cur-mPEC-6	60	10	6:1	-	-	-	-
3	Cur-mPEC-8	80	10	8:1	33.6	144	1.38	-11.3
4	Cur-mPEC-10	100	10	10:1	38.3	158	1.21	-11.8
5	Cur-mPEC-12	120	10	12:1	41.2	182	1.18	-12.4
6	Cur-mPEC-15	150	10	15:1	-	-	-	-

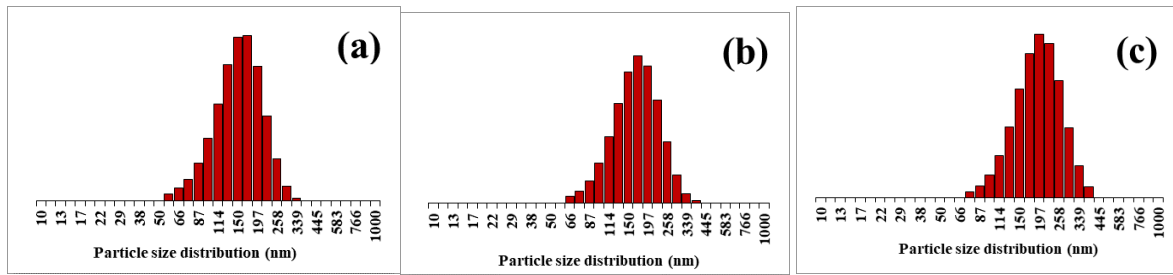


Figure 2. Particle size distributions of (a) Cur-mPEC-8, (b) Cur-mPEC-10, and (c) Cur-mPEC-12.

Table 2. Compositions of Cur-mPEC-C composites.

No.	Chitosan (g)	Cur-mPEC micelle (g)	% Curcumin	Abbreviation
1	2	0.1	0.005	0.5-cur-mPEC-C
2	2	0.2	0.01	1-cur-mPEC-C
3	2	0.7	0.03	3-cur-mPEC-C
4	2	2.5	0.05	5-cur-mPEC-C

Characterization of Cur-mPEC-C Nanocomposites

Cur-mPEC polymeric micelles have a PCL core that can incorporate hydrophobic drugs and release them by means of either dilution-induced collapse or degradation of micelle-forming polymers. mPEC is known as a highly hydrophilic polymer that can limit drugs' delivery efficiency¹⁷. Hence, chitosan is incorporated into drug-polymeric micelles to maintain the cur-mPEC micelles

as much as possible. In this study, the amount of chitosan was kept constant, while the weight percentage of curcumin was changed by increasing the weight of micelles (mPEC/curcumin mass ratio was 8:1) (Table 2). This current composite membrane contained 0.005, 0.01, 0.03, and 0.05% curcumin, corresponding to 10, 20, 60, and 100 mg of curcumin in 2 g of chitosan. The findings are consistent with a previous study.

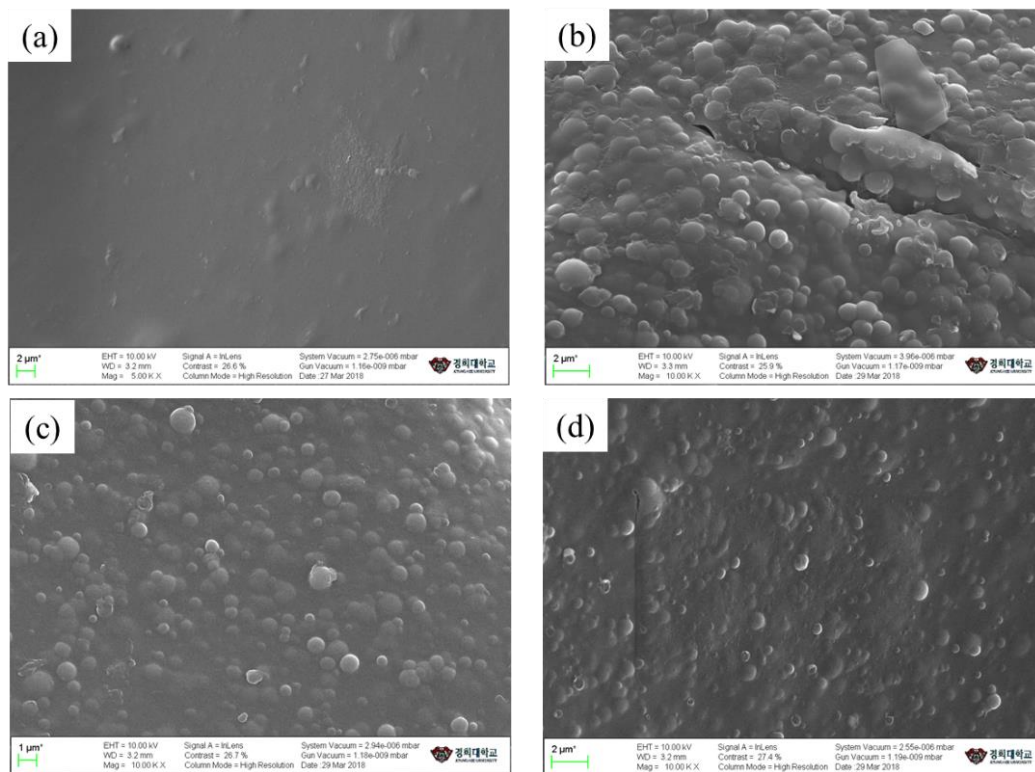


Figure 3. SEM images of (a) chitosan, (b) 0.5-cur-mPEC-C, (c) 1-cur-mPEC-C, and (d) 3-cur-mPEC-C.

Figure 3 exhibits the morphologies of chitosan and chitosan-containing cur-mPEC micelles. As shown, the surface of chitosan was smooth and there were no cracks on the surface (Figure 3a). Meanwhile, the presence of cur-mPEC caused changes in the surface of composites. Obviously, the surface of chitosan became rougher and more micelles were mixed (Figures 3b-d).

Figure 4 shows the FT-IR analyses of the prepared samples. The characteristic bands of curcumin are shown in Figure 4a. The peak at 3508 cm^{-1} was assigned to the O-H stretching of a phenolic hydroxyl group. The specific peaks of C=C stretching and the C=C bend of benzene were shown at wavenumbers 1602 cm^{-1} and 1512 cm^{-1} , respectively²¹. The FT-IR spectrum of mPEC (Figure 4b) demonstrated that the peak of C-H stretching ($\sim 2944\text{ cm}^{-1}$) and C=O stretching band ($\sim 1722\text{ cm}^{-1}$) were attributed to the PCL segments in the copolymer. Moreover, a peak at 1106 cm^{-1} was

assigned to the C-O-C bond of the repeated $-\text{OCH}_2\text{CH}_2-$ units of methoxy poly(ethylene glycol) (mPEG)^{20,28}. The strong broad peaks between 3200 and 3570 cm^{-1} were attributed to stretching of the O-H bond that formed the hydrogen bridges between water and chitosan (Figure 4d). The peak at 1650 cm^{-1} corresponded to the stretching mode of the amide I group in chitosan, which agrees with previous reports^{17,29}. It is clear that all the specific peaks of micelles and chitosan appeared in the FT-IR spectrum of the cur-mPEC-chitosan composite (Figure 4b). It was noted that when the amount of chitosan was much larger than that of the micelles, the peaks at 3546 and 3508 cm^{-1} , as well as the peak at 2944 cm^{-1} , were not observed. Notably, the shift of the C=O vibration from 1722 to 1512 cm^{-1} evidenced that the drug was successfully loaded onto the mPEC micelles. As shown in Figure 4, the peaks at 1000 - 1300 cm^{-1} became stronger and sharper due to the incorporation of cur-mPEC in chitosan.

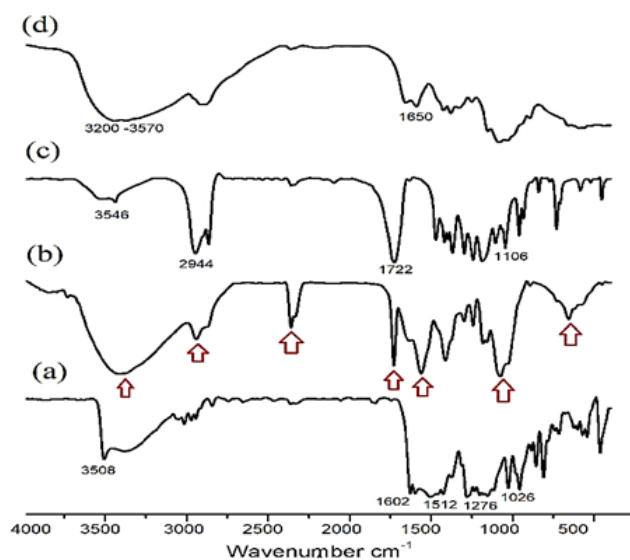


Figure 4. FT-IR spectra of (a) curcumin, (b) cur-mPEC-chitosan composite, (c) mPEC, and (d) chitosan. Arrows indicate the characteristic peaks of micelles and chitosan.

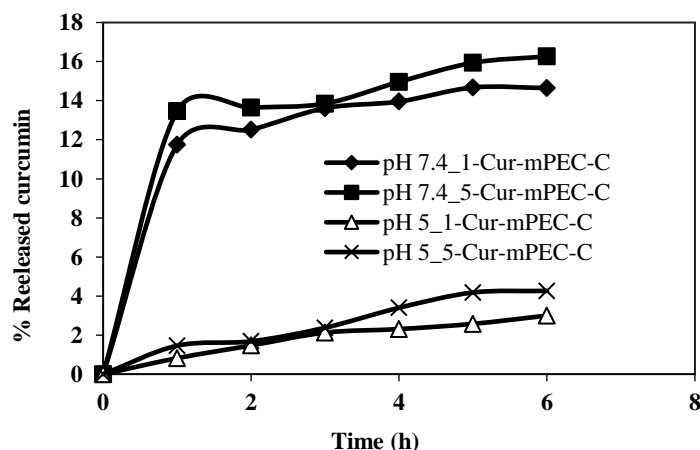


Figure 5. Release profiles of curcumin from cur-mPEC-C nanocomposites at pH = 7.4 and 5.0

Drug Release Profile

According to the literatures^{21,30}, chemical and biochemical factors strongly affect the release of curcumin from the carriers. As shown in Figure 5, the amount of curcumin released from the nanocomposite increased significantly as the pH increased from 5 to 7.4. This is because the solubility of curcumin increases as the pH value increases. It is worth noting that no burst release phenomena were observed at pH 5. This could be explained by the fact that chitosan solubility is limited at lower pH values²⁴, resulting in a longer release time of curcumin^{31,32}. Furthermore, as the amount of micelles in nanocomposites increases, the amount of curcumin released increases.

CONCLUSION

The curcumin-loaded mPEC/chitosan nanocomposites were successfully synthesized by employing the freeze-drying method. The results indicated that curcumin was effectively encapsulated in the prepared micellar nanoparticles. The optimized copolymer/curcumin was 8:1, which had a particle size of ~144 nm. The *in vitro* drug release profile revealed that the release of curcumin was effectively controlled by adjusting the pH value, and there was no burst release of curcumin at pH = 5. These findings imply that the prepared mPEC/chitosan nanocomposite could be a promising curcumin delivery system.

ACKNOWLEDGMENT

The authors would like to thank Ho Chi Minh City University of Food Industry for the financial support. The authors also thank Mis Quynh Mai for her help in manuscript preparation.

DECLARATION OF INTEREST

The authors declare they have no conflict of interest.

REFERENCES

1. Pescosolido, N., Giannotti, R., Plateroti, A. M., Pascarella, A. and Nebbioso, M. (2014) Curcumin: Therapeutic potential in ophthalmology. *Planta Medica*, **80**, 249–254.
2. Nguyen, V. C., Nguyen, V. B. and Hsieh, M. F. (2013) Curcumin-loaded chitosan/gelatin composite sponge for wound healing application. *International Journal of Polymer Science*, **2013**, Article ID 106570.
3. Sun, Y. M., Zhang, H. Y., Chen, D. Z. and Liu, C. B. (2002) Theoretical elucidation on the anti-

- oxidant mechanism of curcumin: A DFT study. *Organic Letters*, **4**, 2909–2911.
4. Hewlings, S. J. and Kalman, D. S. (2017) Curcumin: A Review of Its Effects on Human Health. *Foods*, **6**, 92.
5. Sharifi-Rad, J., Rayess, Y. El, Rizk, A. A., Sadaka, C., Zgheib, R., Zam, W., Sestito, S., Rapposelli, S., Neffe-Skocińska, K., Zielińska, D., Salehi, B., Setzer, W. N., Dosoky, N. S., Taheri, Y., El Beyrouthy, M., Martorell, M., Ostrander, E. A., Suleria, H. A. R., Cho, W. C., Maroyi, A. and Martins, N. (2020) Turmeric and Its Major Compound Curcumin on Health: Bioactive Effects and Safety Profiles for Food, Pharmaceutical, Biotechnological and Medicinal Applications. *Frontiers in pharmacology*, **11**, 1021.
6. Sun, A., Shoji, M., Lu, Y. J., Liotta, D. C. and Snyder, J. P. (2006) Synthesis of EF24-tripeptide chloromethyl ketone: A novel curcumin-related anticancer drug delivery system. *Journal of Medicinal Chemistry*, **49**, 3153–3158.
7. Aggarwal, B. B., Shishodia, S., Takada, Y., Banerjee, S., Newman, R. A., Bueso-Ramos, C. E. and Price, J. E. (2005) Curcumin suppresses the paclitaxel-induced nuclear factor- κ B pathway in breast cancer cells and inhibits lung metastasis of human breast cancer in nude mice. *Clinical Cancer Research*, **11**, 7490–7498.
8. Somasundaram, S., Edmund, N. A., Moore, D. T., Small, G. W., Shi, Y. Y. and Orłowski, R. Z. (2002) Dietary Curcumin Inhibits Chemotherapy-induced Apoptosis in Models of Human Breast Cancer Dietary Curcumin Inhibits Chemotherapy-induced Apoptosis in Models of Human. *Cancer Research*, **62**, 3868–3875.
9. Khezri, K., Saeedi, M., Mohammadamini, H. and Zakaryaei, A. S. (2021) A comprehensive review of the therapeutic potential of curcumin nano-formulations. *Phytotherapy Research*, **35**, 5527–5563.
10. Naksuriya, O., van Steenberg, M. J., Torano, J. S., Okonogi, S. and Hennink, W. E. (2016) A Kinetic Degradation Study of Curcumin in Its Free Form and Loaded in Polymeric Micelles. *The AAPS Journal*, **18**, 777–787.
11. Esatbeyoglu, T., Huebbe, P., Ernst, I. M. A., Chin, D., Wagner, A. E. and Rimbach, G. (2012) Curcumin-from molecule to biological function. *Angewandte Chemie - International Edition*, **51**, 5308–5332.

12. Anand, P., Kunnumakkara, A. B., Newman, R. A. and Aggarwal, B. B. (2007) Bioavailability of curcumin: Problems and promises. *Molecular Pharmaceutics*, **4**, 807–818.
13. Ryall, C., Duarah, S., Chen, S., Yu, H. and Wen, J. (2022) Advancements in Skin Delivery of Natural Bioactive Products for Wound Management: A Brief Review of Two Decades. *Pharmaceutics*, **14**, 1072.
14. Rizvi, S. A. A. and Saleh, A. M. (2018) Applications of nanoparticle systems in drug delivery technology. *Saudi pharmaceutical journal : SPJ : the official publication of the Saudi Pharmaceutical Society*, **26**, 64–70.
15. Abd El-Hack, M. E., El-Saadony, M. T., Swelum, A. A., Arif, M., Abo Ghanima, M. M., Shukry, M., Noreldin, A., Taha, A. E. and El-Tarabily, K. A. (2021) Curcumin, the active substance of turmeric: its effects on health and ways to improve its bioavailability. *Journal of the Science of Food and Agriculture*, **101**, 5747–5762.
16. Nguyen, V. V. L., Pham, G. Q. N., Nguyen, T. H. A. and Nguyen, V. C. (2022) Fabrication and Characterization of Alginate Hydrogels for Control Release System of Catechin-Derived Tea Leave Extract. *Journal of Biomimetics, Biomaterials and Biomedical Engineering*, **58**, 97–107.
17. Letchford, K., Liggins, R. and Burt, H. (2008) Solubilization of hydrophobic drugs by methoxy poly(ethylene glycol)-block-polycaprolactone diblock copolymer micelles: Theoretical and experimental data and correlations. *Journal of Pharmaceutical Sciences*, **97**, 1179–1190.
18. Bernkop-Schnürch, A. and Dünnhaupt, S. (2012) Chitosan-based drug delivery systems. *European Journal of Pharmaceutics and Biopharmaceutics*, **81**, 463–469.
19. Huang, J., Ratnayake, J., Ramesh, N. and Dias, G. J. (2020) Development and Characterization of a Biocomposite Material from Chitosan and New Zealand-Sourced Bovine-Derived Hydroxyapatite for Bone Regeneration. *ACS Omega*, **5**, 16537–16546.
20. Yoshida, C., Uchida, Y., Ito, T., Takami, T. and Murakami, Y. (2017) Chitosan gel sheet containing polymeric micelles: Synthesis and gelation properties of PEG-grafted chitosan. *Materials*, **10**, 1–13.
21. Cuong, N. -Van, Hsieh, M. -Fa, Chen, Y. -T. and Liao, I. (2010) Synthesis and characterization of PEG-PCL-PEG Triblock copolymers as carriers of doxorubicin for the treatment of breast cancer. *Journal of Applied Polymer Science*, **117**, 3694–3703.
22. Elgadir, M. A., Uddin, M. S., Ferdosh, S., Adam, A., Chowdhury, A. J. K. and Sarker, M. Z. I. (2015) Impact of chitosan composites and chitosan nanoparticle composites on various drug delivery systems: A review. *Journal of food and drug analysis*, **23**, 619–629.
23. Sharma, K., Agrawal, S. S. and Gupta, M. (2012) Development and validation of UV spectrophotometric method for the estimation of curcumin in bulk drug and pharmaceutical dosage forms. *International Journal of Drug Development and Research*, **4**, 375–380.
24. Danafar, H., Davaran, S., Rostamizadeh, K., Valizadeh, H. and Hamidi, M. (2014) Biodegradable m-PEG/PCL core-shell micelles: Preparation and characterization as a sustained release formulation for curcumin. *Advanced Pharmaceutical Bulletin*, **4**, 501–510.
25. Yuan, Q., Shah, J., Hein, S. and Misra, R. D. K. (2010) Controlled and extended drug release behavior of chitosan-based nanoparticle carrier. *Acta Biomaterialia*, **6**, 1140–1148.
26. Mahmood, S., Bhattarai, P., Khan, N. R., Subhan, Z., Razaque, G., Albarqi, H. A., Alqahtani, A. A., Alasiri, A. and Zhu, L. (2022) An Investigation for Skin Tissue Regeneration Enhancement/Augmentation by Curcumin-Loaded Self-Emulsifying Drug Delivery System (SEDDS). *Polymers*, **14**, 2904.
27. Ali, M., Khan, N. R., Subhan, Z., Mehmood, S., Amin, A., Rabbani, I., -Rehman, F. -U., Basit, H. M., Syed, H. K., Khan, I. U., Khan, M. S. and Khattak, S. (2022) Novel Curcumin-Encapsulated α -Tocopherol Nanoemulsion System and Its Potential Application for Wound Healing in Diabetic Animals. *BioMed research international*, **2022**, 7669255.
28. Li, Y. -L., Van Cuong, N. and Hsieh, M. -F. (2014) Endocytosis pathways of the folate tethered star-shaped PEG-PCL micelles in cancer cell lines. *Polymers*, **6**, 634–650.
29. Owen, S. C., Chan, D. P. Y. and Shoichet, M. S. (2012) Polymeric micelle stability. *Nano Today*, **7**, 53–65.
30. Cheng, C. Y., Pho, Q. H., Wu, X. Y., Chin, T. Y., Chen, C. M., Fang, P. H., Lin, Y. C. and Hsieh, M. F. (2018) PLGA microspheres loaded with β -cyclodextrin complexes of epigallocatechin-3-gallate for the anti-inflammatory properties in activated microglial cells. *Polymers*, **10**, 519.

31. Mahata, D., Nag, A., Nando, G. B., Mandal, S. M. and Franco, O. L. (2018) Self-Assembled Tea Tannin Graft Copolymer as Nanocarriers for Antimicrobial Drug Delivery and Wound Healing Activity. *J. Nanosci. Nanotechnol.*, **18**, 2361–2369.
32. Tamboli, V., Mishra, G. P. and Mitra, A. K. (2013) Novel pentablock copolymer (PLA-PCL-PEG-PCL-PLA)-based nanoparticles for controlled drug delivery: Effect of copolymer compositions on the crystallinity of copolymers and in vitro drug release profile from nanoparticles. *Colloid and Polymer Science*, **291**, 1235–1245.